

# Mutations of *PKD1* in ADPKD2 cysts suggest a pathogenic effect of *trans*-heterozygous mutations

Autosomal dominant polycystic kidney disease (ADPKD) is caused by mutations in *PKD1* and *PKD2*. The products of these genes associate to form heteromeric complexes. Several models have been proposed to explain the mechanism of cyst formation. Here we find somatic mutations of *PKD2* in 71% of ADPKD2 cysts analysed. Clonal somatic mutations of *PKD1* were identified in a subset of cysts that lacked *PKD2* mutations.

Molecular genetic studies of human cystic tissues suggest a 'two-hit' model of cystogenesis in ADPKD, consistent with the results of gene-targeting studies in mice<sup>1-6</sup>. This model is not universally accepted, however, as loss of heterozygosity (LOH) has been observed in a small fraction of cysts and expression studies have shown upregulation of *PKD1* mRNA and protein in cystic tissue<sup>7-9</sup>.

We reasoned that the detection rate of somatic and germline mutations should be equal if the former are essential for cyst formation. We extended our study of ADPKD2 tissues from patients UT1270 and JHU496 to include all 15 exons and flanking splice junctions of *PKD2* and

found somatic mutations in 71% of the cysts examined (Table 1; refs 5,10,11). The mutations were randomly distributed and no two were identical. In ten cysts we were able to show that the wild-type *PKD2* allele had acquired the mutation.

As polycystin-1 and -2 are closely linked in a common signalling pathway, we hypothesized that somatic *PKD1* mutations might occur in a subset of ADPKD2 cysts<sup>12</sup>. We therefore screened ADPKD2 cysts from UT1270, JHU496 and UT1500 for intragenic *PKD1* mutations. We focused on the replicated region of *PKD1* (exons 2-37) because only a small amount of DNA could be harvested from each cyst<sup>2,13,14</sup>. We attempted to analyse the DNA of the same cysts that had been evaluated in the first part of this study, but this was not uniformly possible due to the variable quality and quantity of cyst DNA. Cysts (C) 1-19 of UT1270 were completely screened for mutations in both genes.

We identified three *PKD2* cysts with somatic *PKD1* mutations (Fig. 1a-e). C15 and C32 of UT1270 had LOH for multiple single-nucleotide polymorphisms (SNPs) in exons 13-15 and 17-20, respectively<sup>14</sup>.

C9 from UT1500 had a nonsense mutation (Q430X) resulting from two adjacent nucleotide substitutions in exon 6 (Fig. 1e). The findings in C32 and C9 were repeated and confirmed using independently amplified templates. In each cyst, comprehensive screening of the entire *PKD2* coding sequence was negative.

We screened in parallel 50 cysts isolated from kidney and liver tissues of people with ADPKD for somatic *PKD2* mutations in the 6 exons (4, 5, 6, 7, 8 and 11) that were reported to have the largest number of germline and somatic mutations<sup>12</sup>. We also examined in each cyst a poly(C) tract (nt 197-203) in exon 1 that was reported to be a hot spot for mutations in *PKD2* (refs 4,15). We did not detect any aberrant variants.

We have shown that somatic *PKD2* mutations can be detected in ADPKD2 cysts at a very high rate if sensitive techniques are used. This finding is consistent with the idea that somatic mutation is an integral step in the pathogenesis of ADPKD. We also identified somatic mutations of *PKD1* in a subset of ADPKD2 cysts that lacked *PKD2* 'second hits'. In the two cysts with LOH for *PKD1*, there was an absence of one *PKD1* allele, implying a clonal origin. This outcome is only possible if the mutation originated at a very early stage in cystogenesis or if it provided a growth advantage. Although we did not find somatic *PKD2* mutations in ADPKD1 organs, we cannot exclude the likelihood that they occur at a low rate, as recently reported<sup>15</sup>.

**Table 1 • Somatic *PKD2* mutations in individual kidney cysts**

Patient ID	Cyst no.	Mutation	Location	Predicted effect	Co-localization with wild-type <i>PKD2</i>
UT1270 (germline <i>PKD2</i> mutation: IVS5±1 G→A; aberrant splicing of exon 5)					
	C2	2050del3	exon 10	del684Y	
	C3	2421insA	exon 13	frameshift 808→811X	
	C4	IVS6-1G→T	exon 7	aberrant splicing of exon 7	
	C5*	1365del13	exon 6	frameshift 455→456X	yes
	C6	1616del2	exon 7	frameshift 538→548X	
	C7	492-495delC	exon 1	frameshift 165→232X	
	C8*	1434del3	exon 6	del479I	yes
	C9*	LOH		loss of normal allele	yes
	C10	1624delC	exon 7	frameshift 542→561X	
	C11*	1450delA	exon 6	frameshift 484→513X	yes
	C14*	1220del34	exon 5	frameshift 407→440X	yes
	C17	IVS9-2del2	exon 10	aberrant splicing of exon 10	
JHU496/NFL 16 (germline <i>PKD2</i> mutation: C1390T; R464X in exon 6)					
	C1*	1510del27	exon 6	del aa 504-512	yes
	C2	IVS8-2A→G	exon 9	aberrant splicing of exon 9	
	C3*	1505insT	exon 6	frameshift 502→525X	yes
	C4	949delA	exon 4	frameshift 318→337X	
	C6	2152-2159InsA	exon 11	frameshift 720→724X	
	C7	IVS+5G→A	exon 6	aberrant splicing of exon 6	yes
	C8*	LOH		loss of normal allele	yes
	C9	1275del5	exon 5	frameshift 426→432X	yes

\*Previously reported<sup>5</sup>.

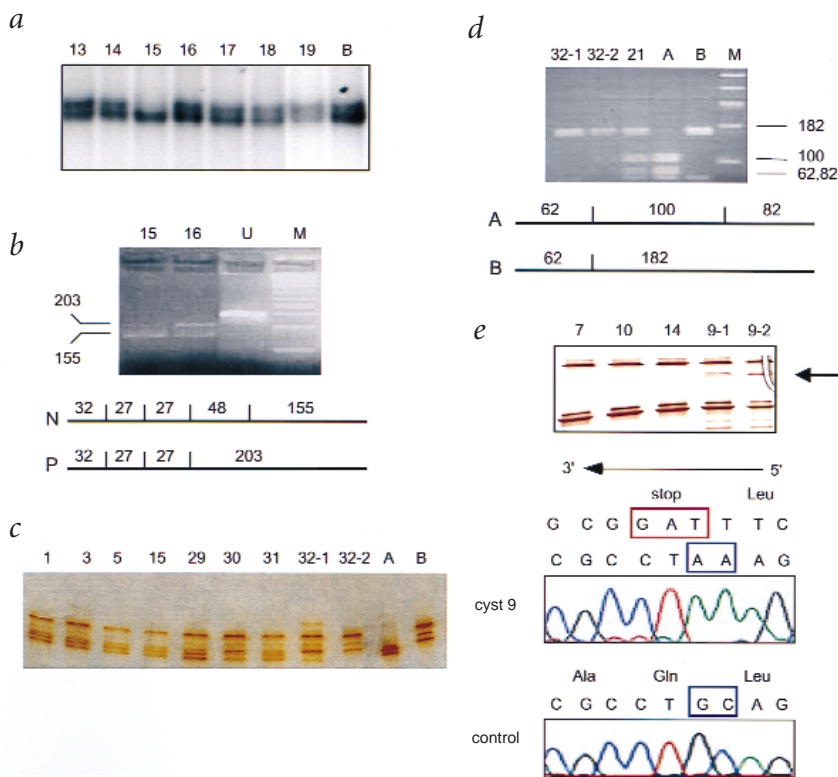


**Fig. 1** Somatic mutations of *PKD1* in *PKD2* cysts. **a**, SSCP analysis of the C5383T SNP in exon 15. A duplex pattern is seen in all samples except C15. C15 also had LOH at another SNP locus in exon 13 (T3274C; data not shown; ref. 14). **b**, Confirmation of LOH by restriction digestion. The C5383T polymorphism (P) results in the loss of an *Hae*III site and creation of a new 203-bp fragment. C15 lacks the 203-bp band compared with a control cyst (C16). **c**, SSCP analysis of the T7376C SNP in exon 17 of UT1270. The SSCP pattern for individuals homozygous for each allele are included (A, B; refs 2, 14). All cysts have both alleles, except C32, which has only B (32-1). This result was confirmed using a second, independently amplified long-range PCR product (32-2). C15, which exhibited LOH for markers in exon 15 (a), is heterozygous for this marker. **d**, Confirmation of LOH in exon 17 by restriction digestion. The T7376C substitution creates a new *Mva*I site in A (present in the control cyst, C21), which is lost in C32-1 and C32-2. U, uncut product; M, 1-kb ladder. **e**, C9 from UT1500 has a 2-bp substitution (G1501T, C1502T; blue box) that results in a premature stop codon (red box). The exon 6 SSCP pattern for four cysts of UT1500 is shown, and the arrow identifies a variant seen in two independent PCR reactions from C9 (9-1, 9-2). The sequence tracings for normal and variant bands are shown in the 3'-5' direction. The complementary sequence is also given with the predicted peptide sequence. Methods for *PKD1* mutation detection have been described<sup>2,13,14</sup>.

Although the scope of our study has been limited by the restricted supply of suitable human tissues, our results suggest that somatic mutation of *PKD1* may be a modifier of disease severity in ADPKD2. We speculate that *trans*-heterozygous loss of function at the somatic level may be sufficient to disrupt the signalling pathway in which these proteins participate.

#### Acknowledgements

We thank the individuals with ADPKD and their families for participation. This work was supported by the NIH (DK48006, DK02562), the Polycystic Kidney Disease Research Foundation and the Kidney Foundation of Canada. G.G.G. is the Irving Blum Scholar of the Johns Hopkins

University School of Medicine.

**Terry Watnick<sup>1\*</sup>, Ning He<sup>2\*</sup>, Kairong Wang<sup>2</sup>, Yan Liang<sup>3</sup>, Patrick Parfrey<sup>4</sup>, Donna Hefferton<sup>4</sup>, Peter St George-Hyslop<sup>3</sup>, Gregory Germino<sup>1</sup> & York Pei<sup>2</sup>**

\*These authors contributed equally to this work.

<sup>1</sup>Department of Medicine, Division of Nephrology, Johns Hopkins University School of Medicine, Baltimore, Maryland, USA.

<sup>2</sup>Department of Medicine, University Health Network, Toronto, Ontario, Canada. <sup>3</sup>Tanz Research Institute, Toronto, Ontario, Canada.

<sup>4</sup>Division of Nephrology, Department of Medicine, Health Sciences Center, St Johns, Newfoundland, Canada. Correspondence should be addressed to G.G. (e-mail: ggermino@welch.jhu.edu) or Y.P. (York.Pei@uhn.on.ca).

1. Qian, F., Watnick, T.J., Onuchic, L.F. & Germino, G.G. *Cell* **87**, 979–987 (1996).
2. Watnick, T.J. *et al.* *Mol. Cell* **2**, 247–251 (1998).
3. Koptides, M., Hadjimichael, C., Koupepidou, P., Pierides, A. & Deltas, C.C. *Hum. Mol. Genet.* **8**, 509–513 (1999).
4. Pei, Y. *et al.* *J. Am. Soc. Nephrol.* **10**, 1524–1529 (1999).
5. Lu, W. *et al.* *Nature Genet.* **17**, 179–181 (1997).
6. Wu, G. *et al.* *Cell* **93**, 177–188 (1998).
7. Geng, L. *et al.* *J. Clin. Invest.* **98**, 2674–2682 (1996).
8. Ong, A.C. *et al.* *Am. J. Pathol.* **154**, 1721–1729 (1999).
9. Ong, A.C. & Harris, P.C. *Lancet* **349**, 1039–1040 (1997).
10. Pei, Y. *et al.* *J. Am. Soc. Nephrol.* **9**, 1852–1860 (1998).
11. Torra, R. *et al.* *Kidney Int.* **56**, 28–33 (1999).
12. Qian, F. *et al.* *Nature Genet.* **16**, 179–183 (1997).
13. Watnick, T.J. *et al.* *Hum. Mol. Genet.* **6**, 1473–1481 (1997).
14. Watnick, T.J. *et al.* *Am. J. Hum. Genet.* **65**, 1561–1571 (1999).
15. Koptides, M., Mean, R., Demetriou, K., Pierides, A. & Deltas, C.C. *Hum. Mol. Genet.* **12**, 447–452 (2000).

## Quantitative mapping of amplicon structure by array CGH identifies *CYP24* as a candidate oncogene

We show here that quantitative measurement of DNA copy number across amplified regions using array comparative genomic hybridization<sup>1–4</sup> (CGH) may facilitate oncogene identification by providing precise information on the locations of both amplicon boundaries

and amplification maxima. Using this analytical capability, we resolved two regions of amplification within an approximately 2-Mb region of recurrent aberration at 20q13.2 in breast cancer. The putative oncogene *ZNF217* (ref. 5) mapped to one peak, and *CYP24* (encoding vitamin D 24

hydroxylase), whose overexpression is likely to lead to abrogation of growth control mediated by vitamin D (ref. 6), mapped to the other.

Positional localization of candidate oncogenes often includes assembly of a contig of large-insert genomic clones, such as BACs, across the region. We have shown previously that such clone sets can be used as probes to map the boundaries of chromosomal rearrangements by fluorescent *in situ* hybridization (FISH) with a finer resolution than the insert size of the clones<sup>7,8</sup>. Here we report that similar sub-clonal resolution mapping of varia-